Inverse inclusion problem: A stable method to determine disks

Faouzi Triki, Chun-Hsiang Tsou

Inverse inclusion problem: A stable method to determine disks

Faouzi Triki[†] and Chun-Hsiang Tsou[‡]

Abstract. In this paper we are interested in inverse inclusion problem in the plane. We derive uniqueness and Hölder stability results of the inclusion recovery problem using a single boundary measurement, under the assumption that the inclusion has a circular shape. We also propose a simple minimizing scheme for the recovery of a disk. Our numerical results show that the Hölder power in the stability estimate is close to one.

1. Introduction

Let Ω be a simply connected Lipschitz domain in $\mathbb{R}^2$, and let D be a subdomain of Ω satisfying $\overline{D} \subset \Omega$. Let $g \in H^{-1/2}(\partial\Omega)$ satisfying $\int_{\partial\Omega} g d\sigma = 0$, fix $k \in \mathbb{R}_+ \setminus \{0, 1\}$, and let $u \in H^1(\Omega)$ be the unique solution to

$$\begin{cases} \operatorname{div}\left((1 + (k-1)\chi_D)\nabla u\right) = 0 & \text{in} \quad \Omega, \\ \dfrac{\partial u}{\partial \nu} = g & \text{on} \quad \partial\Omega, \\ \int_{\partial\Omega} u(x) d\sigma_x = 0, \end{cases} \tag{1.1}$$

where χ_D is the characteristic function of the inclusion D and k is the value of a physical parameter in D (electric or thermal conductivity for example). The inverse inclusion problem is to recover D from the knowledge of a finite number of Cauchy pairs $(g, u)|_{\partial\Omega}$. This inverse problem has a main application in medical imaging, but variants are used in geophysics and other domains. In medical imaging this problem is known under the name of electrical impedance tomography, which is a method of imaging the interior of a body by measurements of current flows and voltages on its surface. On the surface one prescribes current sources g and measures voltage $u|_{\partial\Omega}$ for some or all positions of these sources.

When an infinite number of Cauchy pairs are available, the associated boundary Dirichlet-to-Neumann operator can assumed to be known, and in this case there is a considerable amount of studies. We refer the reader to the survey papers [**13, 1**], and to the books [**9, 5**]. As it is not possible in any concrete experiment to have the access to infinitely many Cauchy pairs, we are interested in recovering the inclusion from a finite number of Cauchy pairs. Assuming that k is known, the question

1991 *Mathematics Subject Classification.* Primary: 35R30.

Key words and phrases. Inverse problems, uniqueness, inclusion, unique continuation, disks, stability estimates.

whether one measurement uniquely determines D has already been addressed in several papers, when D is a ball or a convex polyhedron in $\mathbb{R}^3$ (see for instance [**7, 4, 10**]). The question of stability has been investigated in the case of disks in [**6**] and [**11**]. Kwon [**12**] has established a real-time scheme to locate the unknown inclusion with the hypothesis that its size is small compared with that of Ω. Other works concern the case of inclusions of small sizes, while knowledge about their number, location and conductivity may be derived from the knowledge of a certain number of generalized polarization tensors (Ammari and Kang [**3**]).

In the first part of this paper, we assume that k is a known fixed constant and we focus on the uniqueness and the stability issues for the inverse inclusion problem when D is a disk centering on X_0 with a radius R. Kang and Seo have previously established a Hölder-type stability estimate under a well-chosen current density for the same problem [**6**]. In this work, we drop the last assumption, i.e. we give a new and a more precise Hölder type stability estimate for any non zero Neumann data g. Moreover, we provide in this work a simple minimizing scheme for the recovery of a disk from a single Cauchy data.

The paper is organized as follows. In section 2, we derive uniqueness and stability results of the inclusion recovery problem using a single measurement, under the assumption that the inclusion has a circular shape. We propose a simple minimizing scheme for the recovery of a disk in section 3. Our numerical simulations in section 4 show that the Hölder stability coefficient in the stability estimate is close to one.

2. Uniqueness and stability estimates

Since k is fixed we further denote u the unique solution to the system (1.1). Let $D = B_R(X_0) \subset \Omega_0$ be the disk of radius R centered at X_0, where $\Omega_0 := \{x \in \Omega | \text{dist}(x, \partial\Omega) > \delta_0\}$ for some small constant $\delta_0 > 0$. As we assume D is a disk, we only need to determine its center X_0 and its radius R from the knowledge of a single Cauchy pair $f = u|_{\partial\Omega}$ and g.

Denoting respectively the solution in the interior of the disk D by u^i, and the solution in the exterior by u^e, the equation (1.1) can also be formulated as follows:

$$
\left\{
\begin{array}{lll}
\triangle u^e = 0 & \text{in} & \Omega \setminus \bar{D} \\
\triangle u^i = 0 & \text{in} & D \\
u^e = u^i & \text{on} & \partial D \\
\dfrac{\partial u^e}{\partial \nu} = k \dfrac{\partial u^i}{\partial \nu} & \text{on} & \partial D \\
\dfrac{\partial u}{\partial \nu} = g & \text{on} & \partial\Omega \\
\int_{\partial\Omega} u^e(x) d\sigma_x = 0. &&
\end{array}
\right. \tag{2.1}
$$

2.1. Integral and complex representations.

2.1.1. *Integral representation.* We introduce the fundamental solution of the Laplace operator in the plane.

$$\Gamma(x) = \frac{1}{2\pi} \log |x|,$$

and the single and double layer potentials defined for $\phi \in H^{-\frac{1}{2}}(\partial D)$ by

$$\mathcal{S}_D\phi(x) = \int_{\partial D} \Gamma(x-y)\phi(y)d\sigma_y \qquad x \in \mathbb{R}^2,$$
$$\mathcal{D}_D\phi(x) = \int_{\partial D} \frac{\partial}{\partial \nu_y}\Gamma(x-y)\phi(y)d\sigma_y \qquad x \in \mathbb{R}^2 \setminus \partial D.$$

Using integration by parts, for $x \in \Omega\backslash\bar{D}$, the solution to (1.1) can be represented in the form:

$$\begin{aligned} u^e(x) =& \int_{\partial\Omega} u(y)\frac{\partial}{\partial \nu_y}\Gamma(x-y) - \frac{\partial u}{\partial \nu}(y)\Gamma(x-y)d\sigma_y \\ & - \int_{\partial D} u(y)\frac{\partial}{\partial \nu_y}\Gamma(x-y) - \frac{\partial u}{\partial \nu}(y)\Gamma(x-y)d\sigma_y \\ =& H(x) + \mathcal{S}_D\frac{\partial u^e}{\partial \nu}(x) - \mathcal{D}_D u^e(x), \end{aligned} \tag{2.2}$$

and, for $x \in D$

$$\begin{aligned} u^i(x) =& \int_{\partial D} u(y)\frac{\partial}{\partial \nu_y}\Gamma(x-y) - \frac{\partial u}{\partial \nu}(y)\Gamma(x-y)d\sigma_y \\ =& -\mathcal{S}_D\frac{\partial u^i}{\partial \nu}(x) + \mathcal{D}_D u^i(x), \end{aligned} \tag{2.3}$$

where the harmonic function H is entirely determined by the Cauchy data (f, g)

$$H(x) = \int_{\partial\Omega} u(y)\frac{\partial}{\partial \nu_y}\Gamma(x-y) - \frac{\partial u}{\partial \nu}(y)\Gamma(x-y)d\sigma_y = \mathcal{D}_\Omega f - \mathcal{S}_\Omega g. \tag{2.4}$$

THEOREM 2.1. *The solution to (2.1) admits the following representation*

$$\begin{cases} u^i(x) = H(x) + \dfrac{1-k}{1+k}(H(x) - H(X_0)) & x \in \overline{D} \\ u^e(x) = H(x) + \dfrac{1-k}{1+k}\left(H(X_0 + \dfrac{R^2(x-X_0)}{\|x-X_0\|^2}) - H(X_0)\right), & x \in \Omega \setminus \overline{D} \end{cases} \tag{2.5}$$

PROOF. With the jump condition on ∂D, we have [**3**]

$$\mathcal{D}_D\phi(x)|_\pm = (\mp\frac{1}{2}I + \mathcal{K}_D)\phi(x) \qquad x \in \partial D,$$

where $\mathcal{K}$ is the Neumann-Poincaré operator defined on $L^2(\partial\Omega)$ by

$$\mathcal{K}_D\phi(x) = \frac{1}{2\pi}\int_{\partial D} \frac{\langle y-x, \nu_y\rangle}{|x-y|^2}\phi(y)d\sigma_y.$$

When D is a disk in $\mathbb{R}^2$ of radius R, the operator $\mathcal{K}$ has a very simple form [**3**]

$$\mathcal{K}_D\phi(x) = \frac{1}{4\pi R}\int_{\partial D} \phi(y)d\sigma_y \qquad \forall x \in \partial D.$$

Using the jump conditions, it follows from (2.2) and (2.3) that

$$u^e(x) = H(x) + \mathcal{S}_D\frac{\partial u^e}{\partial \nu}(x) + (\frac{1}{2}I - \mathcal{K}_{\mathcal{D}})u^e(x), \tag{2.6}$$

and

$$u^i(x) = -\mathcal{S}_D\frac{\partial u^i}{\partial \nu}(x) + (\frac{1}{2}I + \mathcal{K}_{\mathcal{D}})u^i(x). \tag{2.7}$$

Adding (2.6) to k times (2.7), and using the mean value propriety for harmonic functions, we obtain for $x \in \partial D$,

$$u(x) = \frac{2}{k+1}H(x) + \frac{2(k-1)}{k+1}\mathcal{K}_D u(x) = \frac{2}{k+1}H(x) + \frac{k-1}{k+1}u^i(X_0).$$

As H is harmonic in D, it follows that u^i coincides with the above right-hand side in $\overline{D}$:

$$u^i(x) = \frac{2}{k+1}H(x) + \frac{k-1}{k+1}u^i(X_0).$$

And, at X_0,

$$u^i(X_0) = \frac{2}{k+1}H(X_0) + \frac{k-1}{k+1}u^i(X_0),$$

which implies $u^i(X_0) = H(X_0)$. Then we have the representation of u^i,

$$u^i(x) = H(x) + \frac{1-k}{1+k}(H(x) - H(X_0)) \qquad x \in \overline{D} \tag{2.8}$$

We represent each point $x \in \Omega$ as $x = X_0 + r\begin{pmatrix}\cos\theta \\ \sin\theta\end{pmatrix}$, with $\theta \in [0, 2\pi)$ and $r > 0$, and we write the function H as a sum of harmonic functions $r^n\cos(n\theta)$ and $r^n\sin(n\theta)$:

$$H(x) = H(X_0) + \sum_{n=1}^{\infty} r^n(a_n\cos(n\theta) + b_n\sin(n\theta)). \tag{2.9}$$

By (2.8) and the transmission conditions, we immediately have:

(2.10)

$$u^i(x) = H(X_0) + \frac{2}{k+1}\sum_{n=1}^{\infty} r^n(a_n\cos(n\theta) + b_n\sin(n\theta)), \qquad x \in D,$$

(2.11)

$$u^e(x) = H(X_0) + \sum_{n=1}^{\infty}(r^n + \frac{1-k}{1+k}(\frac{R^2}{r})^n)(a_n\cos(n\theta) + b_n\sin(n\theta)), \qquad x \in \Omega \setminus \bar{D}.$$

Let $\Psi_D(x)$ denote the point obtained by reflecting x over ∂D

$$\Psi_D(x) = X_0 + \frac{R^2(x - X_0)}{\|x - X_0\|^2} \qquad x \in \mathbb{R}^2 \setminus \{X_0\}.$$

We can thus write

$$u^e(x) = H(x) + \frac{1-k}{1+k}(H(\Psi_D(x)) - H(X_0)) \qquad x \in \Omega \setminus \bar{D}, \tag{2.12}$$

which concludes the proof. □

2.1.2. *Analysis in complex variables.* Using the representation (2.5) of u^e and u^i, we study our problem in the complex plane $\mathbb{C}$. We introduce a harmonic conjugate G of the harmonic function H, so that the function $F := H + iG$ is holomorphic in Ω. Also, the reflection has an explicit expression in terms of complex variables:

$$\Psi_D(z) = Z_0 + \frac{R^2}{\bar{z} - \bar{Z_0}} \qquad z \in \mathbb{C} \setminus \{Z_0\}.$$

By (2.12) and (2.1), the function $H \circ \Psi_D$ is harmonic in $\Omega \setminus \bar{D}$. We can also express its harmonic conjugate $\tilde{G}$ for $x \in \Omega \setminus \bar{D}$ as

$$\begin{aligned} \nabla \tilde{G}(x) &= A \nabla H \circ \Psi_D(x) \\ &= A \mathcal{D}\Psi_D(x) \nabla H(\Psi_D(x)), \end{aligned} \tag{2.13}$$

where $A = \begin{pmatrix} 0 & -1 \\ 1 & 0 \end{pmatrix}$,
and where

$$\mathcal{D}\Psi_D(x) = \frac{R^2}{\|x - X_0\|^2} \begin{pmatrix} (x-X_0)_2{}^2 - (x-X_0)_1{}^2 & -2(x-X_0)_1(x-X_0)_2 \\ -2(x-X_0)_1(x-X_0)_2 & (x-X_0)_1{}^2 - (x-X_0)_2{}^2 \end{pmatrix}.$$

Notice that

$$\mathcal{D}\Psi_D = -\mathcal{D}\Psi_D A,$$

combined with (2.13), which yield:

$$\begin{aligned} \nabla \tilde{G}(x) &= A \nabla H \circ \Psi_D(x) \\ &= A \mathcal{D}\Psi_D(x) \nabla H(\Psi_D(x)) \\ &= -\mathcal{D}\Psi_D(x) A \nabla H(\Psi_D(x)) \\ &= -\mathcal{D}\Psi_D(x) \nabla G(\Psi_D(x)) \\ &= -\nabla G \circ \Psi_D(x). \end{aligned}$$

Thus, the function $-G \circ \Psi_D$ is a harmonic conjugate of the function $H \circ \Psi_D$, and therefore the function $z \mapsto H \circ \Psi_D(z) - iG \circ \Psi_D(z) = \bar{F} \circ \Psi_D(z)$ is holomorphic and its real part is equal to $H \circ \Psi_D$.
Assuming that F is analytic in Ω, we can write F as a sum

$$F(z) = \sum_{n=0}^{\infty} c_n (z - Z_0)^n, \qquad z \in \Omega.$$

Also, the holomorphic function $\bar{F} \circ \Psi_D$ admits the following development:

$$\bar{F} \circ \Psi_D(z) = \sum_{n=0}^{\infty} \bar{c}_n \frac{R^{2n}}{(z - Z_0)^n}, \qquad z \in \Omega \setminus \bar{D}. \tag{2.14}$$

Therefore, denoting by v^e a harmonic conjugate of u^e, and given any $C \in \mathbb{R}$, the function:

$$h(z) := u^e(z) + iv^e(z) = F(z) + \frac{1-k}{1+k}(\bar{F} \circ \Psi_D(z) - H(Z_0) + iC), \qquad z \in \Omega \setminus \bar{D},$$

is holomorphic.

2.2. Uniqueness and stability estimate. We next derive uniqueness and Hölder-type stability estimate for the recovery of the center and radius of the disk. Let D_1, D_2 denote 2 disks centered at the points z_1, z_2 and with radii R_1, R_2. For $i = 1, 2$, let u_i be the solutions of the problem (1.1). We assume that the two solutions satisfy the same non-zero Neumann data g on $\partial\Omega$, and that the L^∞ -norm of the difference between their traces on $\partial\Omega$ (the Dirichlet data) is a small quantity ε. We denote by Ω_1, Ω_2 the images of $\mathbb{C} \setminus \bar{\Omega}$ by the reflections Ψ_{D_1}, Ψ_{D_2}.

THEOREM 2.2. *If $u_1 = u_2$ on $\partial\Omega$, then $D_1 = D_2$.*

PROOF. From (2.4), the function H linked to each solution of (1.1) depends uniquely on the Cauchy data. As u_1 and u_2 have the same Cauchy data, their functions H are the same, and we will note this function by H in this proof.
Using the unique continuation propriety, we have: $u_1 = u_2$ in $\Omega \setminus (D_1 \cup D_2)$.

Case 1: $D_1 \cap D_2 = \emptyset$. In this case, u_1^e has a harmonic continuation in D_1, which coincides with u_2^e i.e. $u_2^e = u_1^i$ in D_1. Then, on ∂D_1, we have:

$$\frac{\partial u_1^i}{\partial \nu} = \frac{\partial u_2^e}{\partial \nu} = \frac{\partial u_1^e}{\partial \nu} = k\frac{\partial u_1^i}{\partial \nu}, \tag{2.15}$$

which implies $\frac{\partial u_1^i}{\partial \nu} = 0$ on ∂D_1, so that $u_1^i = 0$, and thus $u_1 = 0$ and $g = 0$.
Hence the contradiction.

Let $z^\star$ and $Z^\star$ be defined as (2.24).
Case 2: $\partial D_1 \cap \partial D_2 \neq \emptyset$. In this case, from (2.24), $\partial D_1 \cap \partial D_2 = \{z^\star, Z^\star\}$. Then, from the continuity of the solutions, we have:

$$u_1^i(z^\star) = u_1^e(z^\star) = u_2^e(z^\star) = u_2^i(z^\star) \tag{2.16}$$

Using (Theorem 2.1), we have $H(z_1) = H(z_2)$ and $u_1^i = u_2^i$ in $D_1 \cap D_2$.
So, on $\partial(D_1 - D_2)$, $u_1 - u_2 = 0$, which implies $u_1^i = u_2^e$ in $D_1 - D_2$. Then, on the arc $D_1 \cap \partial D_2$, we have:

$$\frac{\partial u_2^i}{\partial \nu} = \frac{\partial u_1^i}{\partial \nu} = \frac{\partial u_2^e}{\partial \nu} = k\frac{\partial u_2^i}{\partial \nu}, \tag{2.17}$$

which implies $\frac{\partial u_1^i}{\partial \nu} = \frac{\partial u_2^i}{\partial \nu} = 0$. For the same reason, we also have: $\frac{\partial u_1^i}{\partial \nu} = \frac{\partial u_2^i}{\partial \nu} = 0$ on the arc $D_2 \cap \partial D_1$. It follows that, $\frac{\partial u_1^i}{\partial \nu} = \frac{\partial u_2^i}{\partial \nu} = 0$ in $\partial(D_1 \cap D_2)$. This also implies $u_1^i = 0$ and then $g = 0$.
Hence the contradiction.

Case 3: $D_1 \subset D_2$. In this case, we have: $z^\star \in D_1$ and $Z^\star \in \mathbb{C} \setminus D_2$. The functions $u_j^e - H$, $j = 1, 2$ have a harmonic extension in $\mathbb{C} \setminus D_2$, and they are equal in $\Omega \setminus D_1$, so from (2.1), we have:

$$H(\Psi_1(z)) - H(z_1) = H(\Psi_2(z)) - H(z_2) \tag{2.18}$$

in $\mathbb{C} \setminus D_2$.
Applying (2.18) on $z^\star$, we have $H(z_1) = H(z_2)$ and then $u_1 = u_2$ in $D_1 \cap D_2 = D_1$.
The rest of the proof follows the same argument as in the previous cases.
That completes the proof □

LEMMA 2.3. *Let $F(z)$ be a non-zero holomorphic function in Ω, and assuming that $D_1 \neq D_2$, then there exists $0 < \beta < 1$, which only depends on F, such that*

$$\int_{\partial\Omega} \frac{|\Psi_1(z) - \Psi_2(z)|}{|F(\Psi_1(z)) - F(\Psi_2(z))|^\beta} ds < \infty. \tag{2.19}$$

PROOF. We first show that the set $\mathcal{Z} := \{z \in \partial\Omega | F(\Psi_1(z)) - F(\Psi_2(z)) = 0\}$ is finite. Indeed, assume that $\mathcal{Z}$ has infinity elements. Then, by an argument of compactness, $\mathcal{Z}$ has a limit point. As the functions $F \circ \Psi_i, i = 1, 2$ are anti-holomorphic, it follows that $F(\Psi_1(z)) = F(\Psi_2(z))$ on $\mathbb{C} \setminus (D_1 \cup D_2)$. Thus, from the explicit formula of solutions, we can construct two solutions to (1.1) related to D_1 and D_2, which have the same Cauchy data on $\partial\Omega$. This contradicts the uniqueness of the inverse problem (Theorem 2.2).

As the function $\mathcal{F}(z) := \overline{F(\Psi_1(z)) - F(\Psi_2(z))}$ is holomorphic in $\mathbb{C} \setminus (D_1 \cup D_2)$, if $\tilde{z} \in \mathcal{Z}$, there is $m(\tilde{z}) \in \mathbb{N}$ such that, in a neighborhood of $\tilde{z}$,

$$\mathcal{F}(z) = \sum_{n \geq m(\tilde{z})} q_n (z - \tilde{z})^n,$$

with $q_{m(\tilde{z})} \neq 0$.
Let $\gamma \in \mathcal{C}^1([a,b])$ be a parametrization of $\partial\Omega$, and set $\tilde{z} = \gamma(\tilde{t})$. Then, in a neighborhood of $\tilde{t}$, we have

$$\mathcal{F}(\gamma(t)) = \sum_{n \geq m(\tilde{z})} q'_n (t - \tilde{t})^n,$$

with $q'_{m(\tilde{z})} \neq 0$.
We choose $0 < \beta < \frac{1}{m}$ where $m := \max_{\tilde{z} \in \mathcal{Z}} m(\tilde{z})$. Then, for $\tilde{t} - \delta < t < \tilde{t} + \delta$ we have,

$$\frac{1}{|\mathcal{F}(\gamma(t))|^\beta} \leq \tilde{C} |t - \tilde{t}|^{-\beta m(\tilde{z})},$$

with $0 < \beta m(\tilde{z}) < 1$.
Therefore,

$$\int_{\tilde{t}-\delta}^{\tilde{t}+\delta} \frac{1}{|\mathcal{F}(\gamma(t))|^\beta} dt < \infty.$$

Thus,

$$\begin{aligned} &\int_{\partial\Omega} \frac{|\Psi_1(z) - \Psi_2(z)|}{|F(\Psi_1(z)) - F(\Psi_2(z))|^\beta} ds \\ &= \int_a^b \frac{|\Psi_1(\gamma(t)) - \Psi_2(\gamma(t))|}{|\mathcal{F}(\gamma(t))|^\beta} |\gamma'(t)| dt < \infty. \end{aligned}$$

and (2.19) follows. □

THEOREM 2.4. *Assume that*

$$\|u_1|_{\partial\Omega} - u_2|_{\partial\Omega}\|_{L^\infty(\partial\Omega)} = \varepsilon. \tag{2.20}$$

Then, there exist constants $0 < \alpha, \beta < 1$ and $C > 0$, such that

$$|z_1 - z_2| \leq C \varepsilon^{\alpha\beta}, \tag{2.21}$$

and

$$|R_1 - R_2| \leq C \varepsilon^{\alpha\beta}, \tag{2.22}$$

where $\alpha := \omega(z^\star) > 0$, and where ω and $z^\star$ are given by the following equations

$$\begin{cases} \triangle \omega = 0 & \text{in } \Omega \setminus \overline{\Omega_1 \cup \Omega_2} \\ \omega = 1 & \text{on } \partial\Omega \\ \omega = 0 & \text{on } \partial(\Omega_1 \cup \Omega_2), \end{cases} \tag{2.23}$$

$$z_1 + \frac{R_1^2}{\bar{z}^\star - \bar{z}_1} = z_2 + \frac{R_2^2}{\bar{z}^\star - \bar{z}_2} = Z^\star \in \mathbb{C}, \tag{2.24}$$

where β only depends on the boundary Cauchy data.

REMARK 2.5. About the location of the points $z^\star$ and $Z^\star$, we observe that

- $Z^\star$ is the image of $z^\star$ by the reflection with respect to ∂D_1 and with respect to ∂D_2.

- in the case where $\partial D_1 \cap \partial D_2 \neq \emptyset$, $z^\star = Z^\star$ is one of the intersection points.
- in the case where $D_1 \cap D_2 = \emptyset$, then either $z^\star \in D_1$ and $Z^\star \in D_2$ or $z^\star \in D_2$ and $Z^\star \in D_1$.
- in the case where $D_1 \subset D_2$ (resp. $D_2 \subset D_1$), then $z^\star \in D_1$ (resp. $z^\star \in D_2$) and $Z^\star \in \mathbb{C} \setminus D_2$ (resp. $Z^\star \in \mathbb{C} \setminus D_1$).
- at least one of the points $z^\star$ and $Z^\star$ is in Ω. We can always assume that $z^\star \in \Omega$.

Proof. According to the position of the point $Z^\star$, we distinguish two cases:
Case 1: both $z^\star$ and $Z^\star$ are in Ω.
Because $Z^\star$ is the image of $z^\star$ by Ψ_{D_1} and vice-versa, one of $z^\star$ or $Z^\star$ is in $\bar{D_1}$, the other lies in $\Omega \setminus D_1$. We may assume that $z^\star \in \Omega \setminus D_1$.
We define
(2.25)

$$\tilde{h}_i(z) = h_i(z) - h_i(z^\star) = F_i(z) - F_i(z^\star) + \frac{1-k}{1+k}\left(\overline{F_i(z_i + \frac{R_i^2}{\bar{z} - \bar{z}_i})} - \overline{F_i(Z^\star)}\right).$$

By construction, the function $h_1 - h_2$ can be holomorphically extended in $\Omega \setminus \overline{\Omega_1 \cup \Omega_2}$ and satisfies

$$M := \sup\{|h_1 - h_2| : z \in \Omega \setminus \overline{\Omega_1 \cup \Omega_2}\} \leq C||g||_{L^2(\partial\Omega)}, \tag{2.26}$$

$$|h_1 - h_2| \leq \varepsilon \qquad \text{on } \partial\Omega. \tag{2.27}$$

Consequently, for $z \in \partial\Omega$,

$$\begin{aligned} &\tilde{h}_1(z) - \tilde{h}_2(z) \\ &= h_1(z) - h_2(z) - [h_1(z^\star) - h_2(z^\star)] \\ &= F_1(z) - F_2(z) + F_1(z^\star) - F_2(z^\star) \\ &+ \frac{1-k}{1+k}\left(\overline{F_1(z_1 + \frac{R_1^2}{\bar{z} - \bar{z}_1})} - \overline{F_2(z_2 + \frac{R_2^2}{\bar{z} - \bar{z}_2})} + \overline{F_2(Z^\star)} - \overline{F_1(Z^\star)}\right). \end{aligned} \tag{2.28}$$

Let ω be the solution to the Dirichlet problem (2.23), the function $\omega \log\varepsilon + (1-\omega)\log M$ is therefore harmonic in $\Omega \setminus \overline{\Omega_1 \cup \Omega_2}$. On the other hand, $\log|h_1 - h_2| = \Re(\log(h_1 - h_2))$ is also a harmonic function in $\Omega \setminus \overline{\Omega_1 \cup \Omega_2}$. From (2.26) and (2.27), we have

$$\log|h_1(z) - h_2(z)| \leq \omega(z)\log\varepsilon + (1-\omega(z))\log M, \qquad z \in \partial(\Omega \setminus \overline{\Omega_1 \cup \Omega_2}) \tag{2.29}$$

Then, by the maximum principle,

$$\log|h_1(z^\star) - h_2(z^\star)| \leq \omega(z^\star)\log\varepsilon + (1-\omega(z^\star))\log M \tag{2.30}$$

Hence,

$$|h_1(z^\star) - h_2(z^\star)| \leq C\varepsilon^\alpha, \tag{2.31}$$

with $\alpha := \omega(z^\star)$.
Using the assumption (2.20) and the definition (2.4) of H, we have

$$\forall z \in \bar{\Omega},\ |F_1(z) - F_2(z)| \leq C\varepsilon. \tag{2.32}$$

Further, from (2.28) we have that for all $z \in \partial\Omega$,

$$\begin{aligned}
&\overline{F_1(z_1 + \frac{R_1^2}{\bar{z} - \bar{z}_1})} - \overline{F_1(z_2 + \frac{R_2^2}{\bar{z} - \bar{z}_2})} \\
&= \overline{F_1(Z^\star)} - \overline{F_2(Z^\star)} + \frac{1+k}{1-k}[F_2(z) - F_1(z) + F_2(z^\star) - F_1(z^\star) \\
&+ h_1(z) - h_2(z) + h_2(^\star) - h_1(z^\star)]. \qquad (2.33)
\end{aligned}$$

Applying (2.27), (2.31) and (2.32), we obtain:

$$|\overline{F_1(z_1 + \frac{R_1^2}{\bar{z} - \bar{z}_1})} - \overline{F_1(z_2 + \frac{R_2^2}{\bar{z} - \bar{z}_2})}| \leq C\varepsilon^\alpha, \qquad \forall z \in \partial\Omega. \qquad (2.34)$$

Then, using (2.34) and (2.19), we have the following estimate:

$$\begin{aligned}
&\int_{\partial\Omega} |\Psi_1(z) - \Psi_2(z)| ds \\
&= \int_{\partial\Omega} \frac{|\Psi_1(z) - \Psi_2(z)|}{|F_1(\Psi_1(z)) - F_1(\Psi_2(z))|^\beta} |F_1(\Psi_1(z)) - F_1(\Psi_2(z))|^\beta ds \\
&\leq \int_{\partial\Omega} \frac{|\Psi_1(z) - \Psi_2(z)|}{|F_1(\Psi_1(z)) - F_1(\Psi_2(z))|^\beta} ds \times C\varepsilon^{\alpha\beta} \\
&\leq C'\varepsilon^{\alpha\beta}. \qquad (2.35)
\end{aligned}$$

On the other hand, we have:

$$\begin{aligned}
&\int_{\partial\Omega} |\Psi_1(z) - \Psi_2(z)| ds \\
&= \int_{\partial\Omega} |\overline{\Psi_1(z) - \Psi_2(z)}| ds \\
&\geq |\int_{\partial\Omega} \overline{\Psi_1(z) - \Psi_2(z)} dz| \\
&= |\int_{\partial\Omega} \bar{z}_1 - \bar{z}_2 + \frac{R_1^2}{z - z_1} - \frac{R_2^2}{z - z_2} dz| \\
&= |R_1^2 - R_2^2|.
\end{aligned}$$

So, we have:

$$|R_1 - R_2| \leq C\varepsilon^{\alpha\beta}. \qquad (2.36)$$

Using (2.36), we have: for all $z \in \partial\Omega$,

$$|\Psi_1(z) - \Psi_2(z)| = |\bar{z}_1 - \bar{z}_2 + R_1^2 \frac{z_1 - z_2}{(z - z_1)(z - z_2)}| + O(\varepsilon^{\alpha\beta}).$$

So, from (2.35),

$$\begin{aligned}
&C\varepsilon^{\alpha\beta} \\
&\geq \int_{\partial\Omega} |\bar{z}_1 - \bar{z}_2 + R_1^2 \frac{z_1 - z_2}{(z - z_1)(z - z_2)}| ds \\
&= |z_1 - z_2| \int_{\partial\Omega} |e^{-2i \arg(z_1 - z_2)} + \frac{R_1^2}{(z - z_1)(z - z_2)}| ds
\end{aligned}$$

with $\displaystyle\int_{\partial\Omega} |e^{-2i\arg(z_1-z_2)} + \frac{R_1^2}{(z-z_1)(z-z_2)}|ds > 0.$
Thus,

$$|z_1 - z_2| \leq C\varepsilon^{\alpha\beta}. \tag{2.37}$$

Case 2: $z^\star \in \Omega$, $Z^\star \in \mathbb{C}\setminus\bar{\Omega}$. We define

$$\tilde{h}_i(z) = h_i(z) - (h_i(Z^\star) - f_i(Z^\star)) = f_i(z) + \frac{1-k}{1+k}\left(\overline{F_i(z_i + \frac{R_i^2}{\bar{z}-\bar{z}_i})} - \overline{F_i(z^\star)}\right). \tag{2.38}$$

By (2.14), the holomorphic functions $h_i - F_i$, $i = 1, 2$ can be extended to $\mathbb{C}\setminus\bar{D}_i$ and they vanish as $|z| \to \infty$. Let $\tilde{\Omega}$ be an open set containing Ω and the point Z^*, and consider a harmonic function ω solution to the following equation

$$\begin{cases} \triangle\omega = 0 & \text{in } \tilde{\Omega}\setminus\bar{\Omega} \\ \omega = 1 & \text{on } \partial\Omega \\ \omega = 0 & \text{on } \partial\tilde{\Omega}. \end{cases} \tag{2.39}$$

Define $\alpha = \omega(Z^\star)$.
Thus, from (2.27) and (2.32) we have

$$|(h_1 - F_1) - (h_2 - F_2)| \leq C\varepsilon \qquad \text{on } \partial\Omega. \tag{2.40}$$

We apply the maximum principle on $\tilde{\Omega}\setminus\Omega$ to the harmonic function $\omega\log\varepsilon + (1-\omega)\log M - \log|(h_1 - F_1) - (h_2 - F_2)|$ to obtain:

$$\log|(h_1 - F_1)(Z^\star) - (h_2 - F_2)(Z^\star)| \leq \omega(Z^\star)\log\varepsilon + (1-\omega(Z^\star))\log M, \tag{2.41}$$

so that

$$|(h_1 - F_1)(Z^\star) - (h_2 - F_2)(Z^\star)| \leq C\varepsilon^{\alpha}. \tag{2.42}$$

In fact, we can choose, $\tilde{\Omega} = B_\rho(z_1)$ with ρ as large as we want. We denote ω_ρ the solution to the associated equation (2.39) and we also consider the harmonic function $\tilde{\omega_\rho}$ solution to

$$\begin{cases} \triangle\tilde{\omega}_\rho = 0 & \text{in } B(z_1,\rho)\setminus B(z_1,R_1) \\ \tilde{\omega}_\rho = 1 & \text{on } \partial B(z_1,R_1) \\ \tilde{\omega}_\rho = 0 & \text{on } \partial B(z_1,\rho). \end{cases} \tag{2.43}$$

The function $\tilde{\omega_\rho}$ has the explicit expression

$$\tilde{\omega}_\rho(r) = \frac{\log(r) - \log(\rho)}{\log(R) - \log(\rho)}, \tag{2.44}$$

with $r := |z - z_1|$.
By the maximum principle, $\tilde{\omega}_\rho \leq \omega_\rho$ in $B(z_1,\rho)\setminus\Omega$. So, we have

$$1 > \omega_\rho(Z^\star) \geq \tilde{\omega}_\rho(Z^\star) = \frac{\log(r) - \log(\rho)}{\log(R) - \log(\rho)} \underset{\rho\to\infty}{\longrightarrow} 1. \tag{2.45}$$

From (2.42), we have

$$|(h_1(Z^\star) - F_1(Z^\star)) - (h_2(Z^\star) - F_2(Z^\star))| \leq C\varepsilon^{\beta}, \qquad 0 < \beta < 1. \tag{2.46}$$

Thus,

$$|(h_1(Z^\star) - F_1(Z^\star)) - (h_2(Z^\star) - F_2(Z^\star))| \leq C\varepsilon. \tag{2.47}$$

The rest of the proof follows the same argument as that of *case 1.* □

2.3. Reconstruction from two measurements. It follows from the analysis of section 2.1.2 that we can obtain some geometric elements of the disk from a simple contour integration. Thus, we can reconstruct the center, the radius and the conductivity k if we have two distinct measures under the assumption that $\nabla u \neq 0$ in Ω. The method of reconstruction is described as follows.
We calculate the following integral:

$$I := \frac{1}{2\pi i}\int_{\partial\Omega} h(z)dz. \tag{2.48}$$

Using the representation (2.14) and the Residue Theorem on Ω, we have

$$\begin{aligned}
I :&= \frac{1}{2\pi i}\int_{\partial\Omega} h(z)dz \\
&= \frac{1}{2\pi i}\int_{\partial\Omega} F(z) + \frac{1-k}{1+k}(\bar{F}\circ\Psi_D(z) - H(Z_0) + iC)dz \\
&= \frac{1}{2\pi i}[\int_{\partial\Omega} F(z)dz + \frac{1-k}{1+k}(\int_{\partial\Omega}\sum_{n=0}^{\infty}\bar{c}_n\frac{R^{2n}}{(z-Z_0)^n}dz + \int_{\partial\Omega} -H(Z_0) + iCdz)] \\
&= \frac{1}{2\pi i}\frac{1-k}{1+k}\sum_{n=1}^{\infty}\bar{c}_n R^{2n}\int_{\partial\Omega}\frac{1}{(z-Z_0)^n}dz \\
&= \frac{1-k}{1+k}\bar{c}_1 R^2 = \frac{1-k}{1+k}\overline{F'(Z_0)}R^2.
\end{aligned} \tag{2.49}$$

Using the same arguments, we can also calculate the following integral

$$\begin{aligned}
&\frac{1}{2\pi i}\int_{\partial\Omega} zh(z)dz = \frac{1}{2\pi i}\int_{\partial\Omega} zF(z) + \frac{1-k}{1+k}z(\bar{F}\circ\Psi_D(z) - H(Z_0) + iC)dz \\
&= \frac{1}{2\pi i}[\int_{\partial\Omega} zF(z)dz + \frac{1-k}{1+k}(\int_{\partial\Omega}\sum_{n=0}^{\infty}\bar{c}_n\frac{zR^{2n}}{(z-Z_0)^n}dz + \int_{\partial\Omega} z(-H(Z_0) + iC)dz)] \\
&= \frac{1}{2\pi i}\frac{1-k}{1+k}\sum_{n=1}^{\infty}\bar{c}_n R^{2n}\int_{\partial\Omega}\frac{z}{(z-Z_0)^n}dz \\
&= \frac{1}{2\pi i}\frac{1-k}{1+k}\sum_{n=1}^{\infty}\bar{c}_n R^{2n}\int_{\partial\Omega}\frac{1}{(z-Z_0)^{n-1}} + \frac{Z_0}{(z-Z_0)^n}dz \\
&= \frac{1-k}{1+k}(Z_0\bar{c}_1 R^2 + \bar{c_2}R^4).
\end{aligned} \tag{2.50}$$

Denoting by f_1, f_2 two functions f corresponding to two distinct measurements, from (2.49) we have

$$\frac{\bar{I}_1}{\bar{I}_2} = \frac{F_1'(Z_0)}{F_2'(Z_0)} \tag{2.51}$$

So, Z_0 is a zero of the holomophic function $z \mapsto \dfrac{F_1'(z)}{F_2'(z)} - \dfrac{\bar{I}_1}{\bar{I}_2}$ ($F_2'(z) \neq 0\,\forall z \in \Omega$ as we supposed that $\nabla u \neq 0$). Once Z_0 is determined, R and k can be easily found from (2.49) and (2.50).

3. Optimization algorithms

In this section, we consider a numerical scheme to reconstruct a disk contained in a subset $\Omega_0 \subset \Omega$ with $\text{dist}(\partial\Omega_0, \partial\Omega) \geq \delta_0 > 0$, using a single measurement. The scheme is based on minimizing the functional

$$J(u) = \frac{1}{2}\int_{\partial\Omega} |u - u_{meas}|^2 d\sigma,$$

where u_{meas} is the measured Dirichlet data and where u is the solution to (1.1) associated to a disk $D = B(X_0, R) \subset \Omega_0$.

Given $(c_1, c_2, R) \in \mathbb{R}^3$, the gradient of the functional J at this point can be calculated as follows.

THEOREM 3.1. *Let u be the solution to the problem (1.1) associated to a disk and let w be the solution to the following problem*

$$\begin{cases} div((1 + (k-1)\chi_D)\nabla w) = 0 & in \quad \Omega, \\ \dfrac{\partial w}{\partial \nu} = u - u_{meas} & on \quad \partial\Omega. \end{cases} \tag{3.1}$$

Then

$$\frac{\partial J}{\partial c_1} = (k-1)\int_D \frac{\partial}{\partial x_1}(\nabla u \nabla w) dX \tag{3.2}$$

$$\frac{\partial J}{\partial c_2} = (k-1)\int_D \frac{\partial}{\partial x_2}(\nabla u \nabla w) dX \tag{3.3}$$

$$\frac{\partial J}{\partial R} = \frac{k-1}{R}\int_D 2\nabla u \nabla w + \sum_{i=1,2}(x_i - c_i)\frac{\partial}{\partial x_i}(\nabla u \nabla w) dX. \tag{3.4}$$

PROOF. Let $(c_1, c_2, R) \in \mathbb{R}^3$, such that the disk D centered at (c_1, c_2), with radius R is included in Ω_0. Denote u (receptively $\tilde{u}$) the solutions to (1.1) associated to the disk $B_R(c_1, c_2)$ (respectively $B_R(c_1 + dx_1, c_2)$). Then we have

$$\begin{aligned} J(c_1 + dc_1, c_2, R) - J(c_1, c_2, R) &= \frac{1}{2}\int_{\partial\Omega} |\tilde{u} - u_{meas}|^2 d\sigma - \frac{1}{2}\int_{\partial\Omega} |u - u_{meas}|^2 d\sigma \\ &= \frac{1}{2}\int_{\partial\Omega} (\tilde{u} - u)(\tilde{u} + u - 2u_{meas}) d\sigma \\ &= \frac{1}{2}\int_{\partial\Omega} (\tilde{u} - u)(\tilde{u} - u + 2(u - u_{meas})) d\sigma \\ &= \int_{\partial\Omega} (u - u_{meas}) v dc_1 d\sigma + O(|dc_1|^2). \end{aligned}$$

Therefore,

$$\frac{\partial J}{\partial c_1} = \int_{\partial\Omega} (u - u_{meas}) v d\sigma, \tag{3.5}$$

where $v := \lim_{dc_1 \to 0} \dfrac{\tilde{u} - u}{dc_1}$.

Combining the variational forms of (1.1) for u and for $\tilde{u}$, we have that for all $\phi \in H^1(\Omega)$,

$$\int_\Omega (1 + (k-1)\chi_{\tilde{D}})\nabla \tilde{u} \nabla \phi dX - \int_{\partial\Omega} g\phi d\sigma = 0, \tag{3.6}$$

and

$$\int_\Omega (1+(k-1)\chi_D)\nabla u\nabla\phi dX - \int_{\partial\Omega} g\phi d\sigma = 0. \tag{3.7}$$

By applying a result of shape derivative (see [**2**]), (3.6)-(3.7) give us:

$$\begin{aligned}
0 &= \frac{1}{dc_1}[\int_\Omega (1+(k-1)\chi_{\tilde{D}})\nabla\tilde{u}\nabla\phi dX - \int_\Omega (1+(k-1)\chi_D)\nabla u\nabla\phi dX] \\
&= \int_\Omega \nabla v\nabla\phi dX + \frac{k-1}{dc_1}(\int_{\tilde{D}} \nabla\tilde{u}\nabla\phi dX - \int_D \nabla u\nabla\phi dX) \\
&= \int_\Omega (1+(k-1)\chi_D)\nabla v\nabla\phi dX + \frac{k-1}{dc_1}(\int_{\tilde{D}} \nabla u\nabla\phi dX - \int_D \nabla u\nabla\phi dX) + O(|dc_1|) \\
&= \int_\Omega (1+(k-1)\chi_D)\nabla v\nabla\phi dX + (k-1)\int_{\partial D} e_1\cdot\nu\nabla u\nabla\phi d\sigma + O(|dc_1|).
\end{aligned}$$

It follows that v satisfies, for all $\phi \in H^1(\Omega)$,

$$\int_\Omega (1+(k-1)\chi_D)\nabla v\nabla\phi dX + (k-1)\int_{\partial D} e_1\cdot\nu\nabla u\nabla\phi d\sigma. \tag{3.8}$$

Introducing the function w defined by (3.1), and taking w as ϕ in (3.8) we get

$$0 = \int_\Omega (1+(k-1)\chi_D)\nabla v\nabla w dX + (k-1)\int_{\partial D} e_1\cdot\nu\nabla u\nabla w d\sigma. \tag{3.9}$$

On the other hand,

$$\begin{aligned}
0 &= \int_\Omega \mathrm{div}[(1+(k-1)\chi_D)\nabla w]v dX \\
&= \int_{\partial\Omega} v(u-u_{meas})d\sigma + \int_\Omega (1+(k-1)\chi_D)\nabla v\nabla w dX.
\end{aligned}$$

Consequently,

$$\frac{\partial J}{\partial c_1} = \int_{\partial\Omega}(u-u_{meas})v d\sigma \tag{3.10}$$

$$= (k-1)\int_{\partial D} e_1\cdot\nu\nabla u\nabla w d\sigma \tag{3.11}$$

$$= (k-1)\int_{\partial D} \frac{\partial x_1}{\partial\nu}\nabla u\nabla w d\sigma \tag{3.12}$$

$$= (k-1)\int_D \frac{\partial}{\partial x_1}(\nabla u\nabla w)dX, \tag{3.13}$$

and (3.2) follows. By the same argument, we can obtain (3.3) and

$$\frac{\partial J}{\partial R} = (k-1)\int_{\partial D}\nabla u\nabla w d\sigma.$$

As D is a disk, we have $\nu = \frac{x-X_0}{R}$ so that the previous integral becomes

$$\begin{aligned}
\int_{\partial D} \nabla u \nabla w d\sigma &= \int_{\partial D} \nu \cdot \nu \nabla u \nabla w d\sigma \\
&= \int_{\partial D} \frac{x - X_0}{R} \cdot \nu \nabla u \nabla w d\sigma \\
&= \frac{1}{2R} \int_{\partial D} \frac{\partial |x - X_0|^2}{\partial \nu} \nabla u \nabla w d\sigma \\
&= \frac{1}{2R} (\int_D \nabla |x - X_0|^2 \nabla (\nabla u \nabla w) dX + \int_D \triangle (|x - X_0|^2) \nabla u \nabla w dX) \\
&= \frac{1}{R} \int_D 2 \nabla u \nabla w + \sum_{i=1,2} (x_i - c_i) \frac{\partial}{\partial x_i} (\nabla u \nabla w) dX,
\end{aligned}$$

and (3.4) follows. □

The expression of the shape derivative is the basis of the following iterative algorithm:

(1) Chose an initial disk $D = B(X_0, R_0)$.
(2) For each iteration, $i > 0$:
   (a) Calculate the solution to (1.1) u_i, associated to the disk $D_i = B(X_i, R_i)$.
   (b) Calculate the shape derivatives $\frac{\partial J}{\partial c_1}$, $\frac{\partial J}{\partial c_2}$, $\frac{\partial J}{\partial R}$
   (c) Update the parameters of the disk $(X_{i+1}, R_{i+1}) = (X_i, R_i) - \delta \nabla J(X_i, R_i)$ with $\delta > 0$.
   (d) If the updated disk is not entirely in Ω or if R becomes negative, reduce the size δ.
(3) When $J(X_i, R_i)$ becomes smaller than a fixed threshold, we stop.

4. Numerical examples

The setting of all numerical tests is as follows:

- We use FreeFem++ for our numerical experiments [**8**].
- Ω is a centered ellipse defined by the equation: $\frac{x_1^2}{4^2} + \frac{x_2^2}{3^2} \leq 1$.
- the conductivity k is a fixed constant, here we set $k = 5$.
- the Neumann data $g := \frac{\partial u}{\partial \nu}$ is defined by: $g = \langle e, \nu \rangle$ on $\partial\Omega$ where $e = \begin{pmatrix} 2 \\ 3 \end{pmatrix}$.
- We use P2 finite elements for the numerical resolution of the PDEs.
- At each iteration, we remesh the domain to adapt to the new predicted position of the disk.

In this subsection, we show three examples according to the disk's size, and its distance to the boundary $\partial\Omega$,

(1) The target is close to the boundary $\partial\Omega$. Figure 1a shows the solution to (1.1) when the target disk is centered at $X_0 = \begin{pmatrix} 2 \\ 0.8 \end{pmatrix}$ and has radius $R = 1$.
(2) The target is apart from the boundary $\partial\Omega$. Figure 1b shows the solution to (1.1) when the target disk is centered at $X_0 = \begin{pmatrix} 0.5 \\ 0.5 \end{pmatrix}$ and has radius $R = 0.7$.

(3) The target has a small size. Figure 1c shows the solution to (1.1) when the target disk is centered at $X_0 = \begin{pmatrix} 2.4 \\ -1.2 \end{pmatrix}$ and has radius $R = 0.3$.

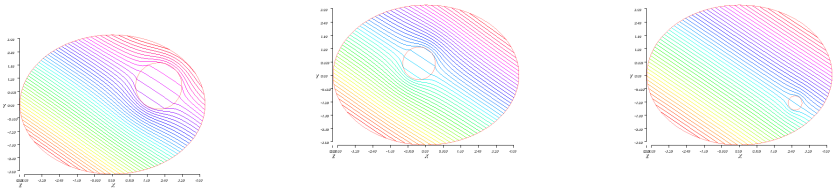

(A) $X_0 = (2, 0.8), R = 1$ (B) $X_0 = (-0.3, 0.5), R = 0.7$ (C) $X_0 = (2.4, -1.2), R = 0.3$

FIGURE 1. Numerical solutions of (1.1)

In these three cases, we exercise our algorithm with the same initial guess: the disk centered at $\begin{pmatrix} 0 \\ 0 \end{pmatrix}$ with radius 2.5.

Figure 2 shows the decay of $\log(J)$ during the iterations in the first case. We can observe that J decays exponentially to 0. To illustrate the dependence between the

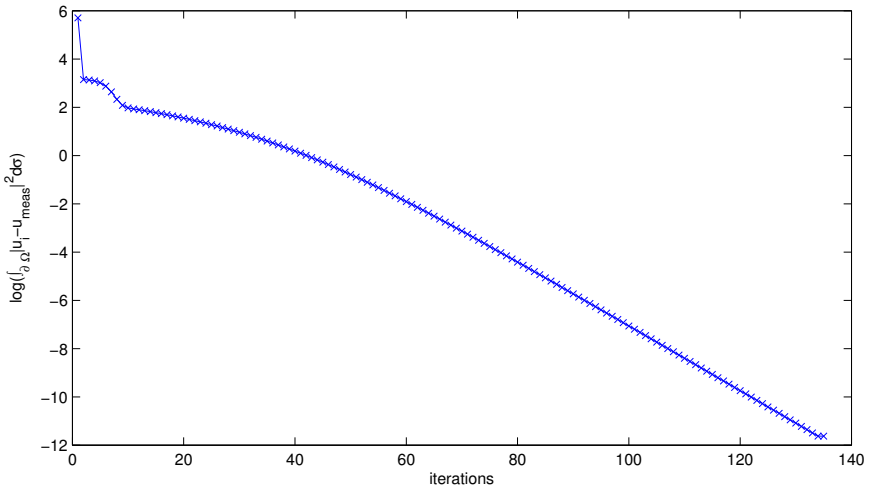

FIGURE 2. Decay of $\log(J)$ during iterations

geometric characteristics of the disk and J, we draw $\log(|X_i - X_0|^2)$ and $\log(|R_i - R_0|^2)$ in terms of $\log(J)$ (Figures 3, 4, 5), where X_i and R_i denote the center and radius of the disk at the i-th iteration. In order to show the Hölder-type stability, it is also interesting to draw linear regression lines to each of these curves. Thus, the inclination of the linear regression lines present a numerical estimation of the Hölder exponent.

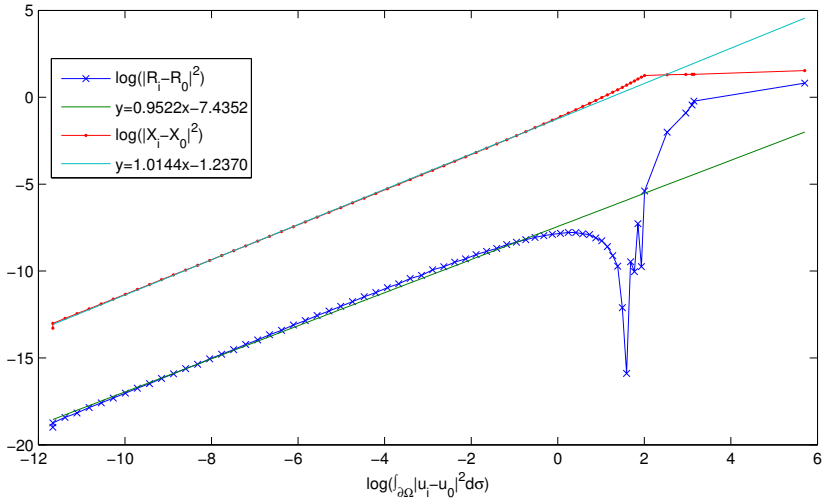

FIGURE 3. Case $X_0 = (2, 0.8)$, $R = 1$

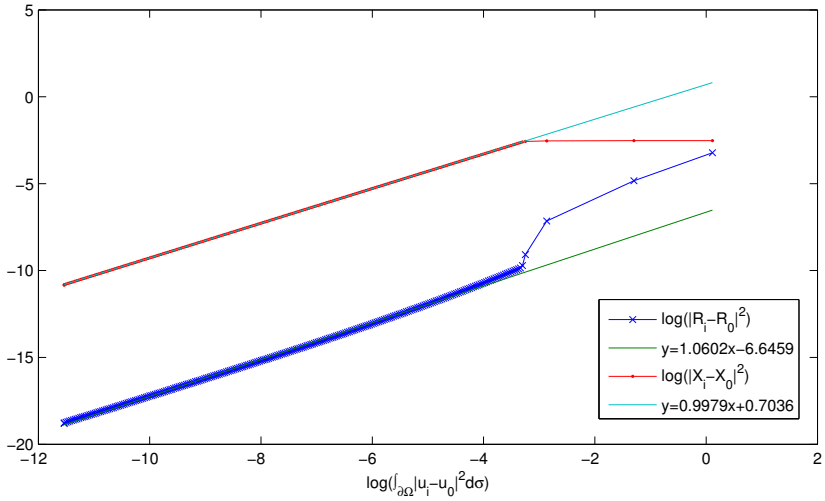

FIGURE 4. Case $X_0 = (-0.3, 0.5)$, $R = 0.7$

Finally, we conclude the numerical results of these three cases by the following observations:

- Figures 3, 4, 5 show the asymptotic behaviors of $|X_i - X_0|$ and $|R_i - R_0|$ when J becomes small. We can observe from the left side of those figures that the data points are very close to a line. That numerically justify the theoretical prediction Theorem 2.4.

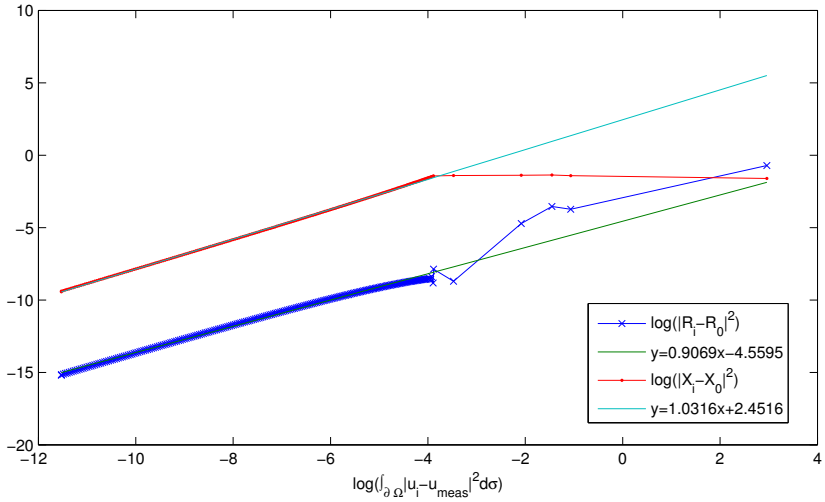

FIGURE 5. Case $X_0 = (2.4, -1.2)$, $R = 0.3$

-The inclination of the linear regression lines present a numerical estimation of the Hölder exponent. Here are the values in those three examples.

	inclination $\log|X_i - X_0|/\log J$	inclination $\log|R_i - R_0|/\log J$
example 1	1.0144	0.9522
example 2	0.9979	1.0602
example 3	1.0316	0.9069

This result shows, the Hölder exponents are all close to 1.

-There is no clear evidence of a relation between the Hölder exponents α and the distance between the target disk and $\partial\Omega$.

-We always choose δ near 0.1. Roughly speaking, when δ exceed 0.5, J does not decay during the iterations.

- For the same target, different initial guesses do not change the number of iterations to reach convergence.

- Exceptionally, if the center of the initial guess coincide with the target's center, only about 10 iterations are needed to reach the target.

- When the target disk is too small, more iterations are needed.

5. Conclusion

We have established the uniqueness of the inclusion recovery problem using a single measurement, under the assumption that the inclusion has a circular shape and we improved the stability estimate result in [**6**]. Our stability estimate is valid even for non-zero input electrical current. Our numerical simulations show that the

Hölder stability coefficient α in the stability estimate is close to 1, which indicates that the dependence might actually be Lipschitz.

6. Acknowledgments

This work has been partially supported by the LabEx PERSYVAL-Lab (ANR-11-LABX- 0025-01).

References

[1] Giovanni Alessandrini. Open issues of stability for the inverse conductivity problem. *Journal of Inverse and Ill-posed Problems jiip*, 15(5):451–460, 2007.
[2] Grégoire Allaire, François Jouve, and Anca-Maria Toader. Structural optimization using sensitivity analysis and a level-set method. *Journal of computational physics*, 194(1):363–393, 2004.
[3] Habib Ammari and Hyeonbae Kang. *Reconstruction of small inhomogeneities from boundary measurements*. Number 1846. Springer Science & Business Media, 2004.
[4] Bartolomé Barceló, Eugene Fabes, and Jin Keun Seo. The inverse conductivity problem with one measurement: uniqueness for convex polyhedra. *Proceedings of the American Mathematical Society*, 122(1):183–189, 1994.
[5] Mourad Choulli. *Une introduction aux problèmes inverses elliptiques et paraboliques*, volume 65. Springer Science & Business Media, 2009.
[6] Eugene Fabes, Hyeonbae Kang, and Jin Keun Seo. Inverse conductivity problem with one measurement: Error estimates and approximate identification for perturbed disks. *SIAM Journal on Mathematical Analysis*, 30(4):699–720, 1999.
[7] Avner Friedman and Victor Isakov. *On the uniqueness in the inverse conductivity problem with one measurement*. Institute for Mathematics and its Applications (USA), 1988.
[8] F. Hecht. New development in freefem++. *J. Numer. Math.*, 20(3-4):251–265, 2012.
[9] Victor Isakov. *Inverse problems for partial differential equations*, volume 127. Springer.
[10] Hyeonbae Kang and Jin Keun Seo. Inverse conductivity problem with one measurement: Uniqueness of balls in $\mathbb{R}^3$. *SIAM Journal on Applied Mathematics*, 59(5):1533–1539, 1999.
[11] Hyeonbae Kang, Jin Keun Seo, and Dongwoo Sheen. The inverse conductivity problem with one measurement: stability and estimation of size. *SIAM Journal on Mathematical Analysis*, 28(6):1389–1405, 1997.
[12] Ohin Kwon, Jin Keun Seo, and Jeong-Rock Yoon. A real time algorithm for the location search of discontinuous conductivities with one measurement. *Communications on Pure and Applied Mathematics*, 55(1):1–29, 2002.
[13] Gunther Uhlmann. Electrical impedance tomography and calderón's problem. *Inverse problems*, 25(12):123011, 2009.

Laboratoire Jean Kuntzmann, UMR CNRS 5224, Université Grenoble-Alpes, 700 Avenue Centrale, 38401 Saint-Martin-d'Hères, France
E-mail address: faouzi.triki@univ-grenoble-alpes.fr

Laboratoire Jean Kuntzmann, UMR CNRS 5224, Université Grenoble-Alpes, 700 Avenue Centrale, 38401 Saint-Martin-d'Hères, France
E-mail address: chun-hsiang.tsou@univ-grenoble-alpes.fr